Earth-Science Reviews 149 (2015) 5–22

Contents lists available at ScienceDirect

Earth-Science Reviews

journal homepage: www.elsevier.com/locate/earscirev

Global warming and the end-Permian extinction event: Proxy and modeling perspectives

Ying Cui *, Lee R. Kump

Department of Geosciences, The Pennsylvania State University, University Park, PA 16802, United States

ARTICLE INFO

Article history:
Received 9 October 2012
Accepted 22 April 2014
Available online 8 May 2014

Keywords:
End-Permian extinction event
Climate model
Geochemical proxies
Temperature
$p\mathrm{CO}_2$

ABSTRACT

The mass extinction event that occurred at the close of the Permian Period (~252 million years ago) represents the most severe biodiversity loss in the ocean of the Phanerozoic. The links between the global carbon cycle, climate change and mass extinction are complex and involve a whole range of often inter-related geochemical, biological, ecologic and climatic factors. It has become widely accepted that the end-Permian mass extinction was associated with a global warming event, because the age of the Siberian Trap eruption, a potentially massive source of carbon dioxide, coincides within error with the extinction event. However, geologic data that are in support of this global warming event are relatively sparse. The chain of events and the causal relationship between the eruption of Siberian Traps and mass extinction is not well established. Global warming, in particular, has only been reported from limited proxy data and climate models, for which the $p\mathrm{CO}_2$ in the atmosphere just before and during the end-Permian extinction event is poorly known. This study critically assesses both the proxy climate data and the existing paleoclimate simulations with the goals of assessing our current understanding of the link between mass extinction and climate change and providing some guidance for future studies. Proxies indicate that prior to the end-Permian extinction event tropical sea surface temperatures ranged from ~22 to 25 °C, and possible $p\mathrm{CO}_2$ values ranged from ~500 to ~4000 ppm before the extinction event. During the peak extinction, tropical temperatures rose up to ~30 °C while $p\mathrm{CO}_2$ perhaps increased up to ~8000 ppm. Climate models that use different pre-event $p\mathrm{CO}_2$ values show similar amount of CO_2 doubling to replicate the observed carbon isotope excursions. We find that the temperature anomaly during the end-Permian extinction is consistent with ~1.5 doublings of atmospheric $p\mathrm{CO}_2$, and that the implied climate sensitivity is 5–6 °C, within the upper range of values produced by climate models.

Contents

---

* Corresponding author at: 512 Deike Building, the Pennsylvania State University, University Park, PA, 16802, United States.
E-mail address: cuiying00@gmail.com (Y. Cui).

http://dx.doi.org/10.1016/j.earscirev.2014.04.007
0012-8252/© 2014 Elsevier B.V. All rights reserved.

1. Introduction

The earth system experienced a series of fundamental upheavals through the Permian–Triassic (P–T) transition (ca. 252 Ma), an interval marked by the largest mass extinction in the geologic record (Burgess et al., 2014; Erwin, 2006). The configuration of the supercontinent Pangea, formed through collision of the southern supercontinent of Gondwana with the northern supercontinent of Laurasia during the late Paleozoic, has been proposed to be responsible for the icehouse to greenhouse transition during the Late Permian (Erwin, 1993). The extent of continental flooding (perhaps reflecting eustatic sea level) reached its minimum during the Late Permian as the supercontinent Pangea was established, leading to extreme continentality (Fig. 1 and reference therein). Reduced availability of fresh silicate rock for weathering due to a long orogenic gap might have caused increased atmospheric CO_2 concentrations and warmed up the Late Permian (Kidder and Worsley, 2004). The pole–equator temperature gradient was probably lower based on the observed high-paleolatitude floras adapted to warm climates (Taylor et al., 1992; Rees et al., 2002). Thick and widespread coals up to the Permian–Triassic boundary (Veevers et al., 1994; Retallack et al., 1996) disappeared for 10 million years, forming a global coal gap. Expansion of subtropical desert belts indicates arid conditions during the Late Permian (Fluteau et al., 2001).

Other lines of evidence, including extremes of the oceanic isotopic compositions of C, S, and Sr suggest that the global environment reached a critical state in the late Paleozoic for which perturbation, namely massive volcanism associated with the eruption of the Siberian Traps, could pitch it over a threshold into near uninhabitability (e.g. Kiehl and Shields, 2005; Erwin, 2006; Luo et al., 2010; Fig. 1). Some researchers have proposed that the end-Permian mass extinction event was a geologically instantaneous catastrophic event (e.g. Bowring et al., 1998; Rampino et al., 2000), but evidence for prolonged extreme environments following the event seems to argue against an instantaneous perturbation (e.g. Romano et al., 2012; Sun et al., 2012). Associated ocean acidification and deoxygenation, similar to that projected for the future, was the likely consequence of volcanic CO_2 emissions and global warming (e.g. Clapham and Payne, 2011; Montenegro et al., 2011; Payne and Clapham, 2012). Following the end-Permian extinction event are widespread microbialite sequences in shallow water settings, reflecting global expansion of microbial ecosystem (Xie et al., 2005, 2007, 2010) and perhaps an anomalously low oceanic sulfate concentration in an anoxic ocean (Luo et al., 2010).

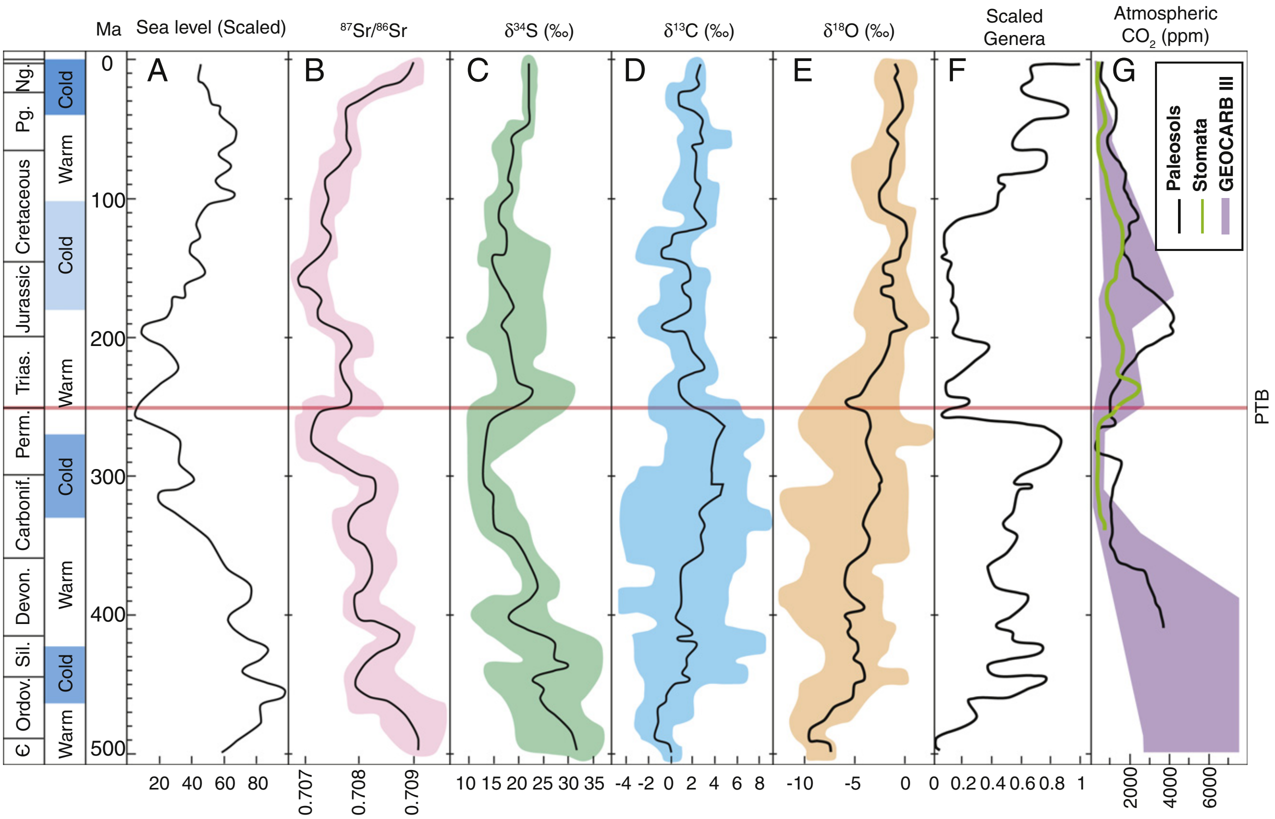

Fig. 1. Long-term environmental variations from the Late Cambrian through the Pliocene. (A) Resampled global continental flooding estimates of 5-million-year bin averages at the bin midpoints of 80 time intervals; (B) to (E) Geochemical analyses from marine carbonates. (F) Total number of marine genera based on North American fossil occurrences; (G) Atmospheric pCO_2 level based on $\delta^{13}C$ of pedogenic carbonate, plant stomatal density and index and GEOCARB III.
Panels (A) to (F) are modified from Hannisdal and Peters (2011). $\delta^{13}C$ and $\delta^{18}O$ records are from low-latitude based on Prokoph et al. (2008). Solid black lines are averages for the time bins used in Hannisdal and Peters (2011), and the shadowed region brackets the data used in Prokoph et al. (2008). Panel (G) is modified from Royer et al. (2004).